Journal of Electron Devices, Vol. 15, 2012, pp. 1291-1295

© JED [ISSN: 1682 -3427]

Journal of Electron Devices
www.jeldev.org

4H-SiC AVALANCHE PHOTODIODES AS UV SENSORS: A BRIEF REVIEW

Moumita Ghosh[1], Mangolika Mondal[2] and Aritra Acharyya[3,†]
[1,2]Supreme Knowledge Foundation Group of Institutions, Sir J. C. Bose School of Engineering, 1, Khan Road, Mankundu, Hooghly, West Bengal - 712139, India.
[3,†]Institute of Radio Physics and Electronics, University of Calcutta, 92, APC Road, Kolkata - 700009, India.
mm.ghosh112@gmail.com[1], mango.mango99@gmail.com[2], ari_besu@yahoo.co.in[3,†]

Received 23/09/2012, online 26-09-2012

ABSTRACT In this paper the potentiality of 4H-SiC Avalanche Photodiodes (APDs) as visible-blind or near visible-blind Ultra-Violet (UV) photodetectors is explored. The first experimental demonstration, investigation of nonlocal effects, single photon detection capability (Geiger mode operation) and study on the effects of electron versus hole photocurrent on opto-electric properties of 4H-SiC APDs are reviewed in brief.
Keywords: 4H-SiC Avalanche Photodiodes, DDR APDs, Nonlocal Effects, Geiger Mode.

I. INTRODUCTION

Avalanche Photodiodes (APDs) are well established high speed, high gain photodetectors. 4H-SiC, a poly-type of SiC (bandgap, E_g = 3.26 eV at 300 K) is one of the most suitable base materials to fabricate APDs for sensing visible-blind or near visible-blind Ultra-Violet (UV) light. 4H-SiC is better base material for UV photodetectors as compared to other promising base material GaN as regards its mature fabrication technology, superior thermo-physical properties and marked difference in the ionization rates of electrons (α_n) and holes (α_p). Yan *et al*. [1] first fabricated p^+-p-n^--n^+ structured reached-through APD (RAPD) and experimentally demonstrated its detection capabilities in 2000. They obtained responsivity of 106 AW^{-1} with optical gain of about 500. Later in 2003, Ng *et al*. [2] investigated the non-local impact ionization effects in 4H-SiC APDs within the wavelength range of 260 – 375 nm. They experimentally obtained peak unity gain responsivity more than 130 mAW^{-1} at 265 nm wavelength with the optical gain of 200 from two types of APD structures (p^+-p-i-n-n^+ and p^+-p-i-n- n^--n^+). Acharyya *et al*. [3] proposed a Double-Drift Region (DDR) APD structure for UV sensing. They carried out the simulation experiment to establish the fact that the 4H-SiC DDR RARD show better opto-electrical characteristics when UV light is incident on the n^+-layer instead of p^+-layer of the p^+-p-n-n^+ structured device and explained this behaviour by the relative values of electron (α_n) and hole (α_p) ionization rates of 4H-SiC.

Several theoretical and experimental studies on homojunction and heterojunction APDs are carried out by different researchers [4-10]. In the present paper the authors have made an attempt to briefly review the significant theoretical and experimental aspects of 4H-SiC APDs.

II. FIRST EXPERIMENTAL DEMONSTRATION

Yan *et al*. [1] first designed and fabricated p^+-p-n^--n^+ structured 4H-SiC visible-blind reach-through avalanche photodiodes with mesa edge termination and thermal oxide passivation techniques. The fabricated devices show "hard" avalanche breakdown. The photo response spectra were measured at different biasing condition and they obtained maximum responsivity of 106 AW^{-1} and corresponding optical gain of about 500. The 4H-SiC RAPDs fabricated by them showed more than 600 times higher peak photo responsivity than that of conventional 6H-SiC photodiodes [11].

III. NONLOCAL EFFECTS IN THIN 4H-SiC UV AVALANCHE PHOTODIODES

B.K. Ng *et al*. [2] investigated the nonlocal impact ionization effects in two thin 4H-SiC APD structures (p^+-p-i-n-n^+ and p^+-p-i-n- n^--n^+) with nominal avalanche width of 0.1 and 0.2 μm. The avalanche multiplication and excess noise characteristics of 4H-SiC APDs with i-region widths of 0.105 and 0.285 μm have been investigated within the wavelength range of 260 – 365 nm; whereas the responsivities of the photo diodes at unity gain were experimented for wavelengths upto 375 μm. They obtained peak unity gain responsivity more than 130 mAW^{-1} at 265 nm wavelength with optical gain of 200 and equivalent quantum efficiency of about 60% from both type of the structures. They also modeled the experimental results using a simple quantum efficiency model and a non-local description yields effective ionization threshold energies of 12 and 8 eV for electrons and holes respectively. It suggests the soft dead space in 4H-SiC. They showed that although dead space is important in 4H-SiC, pure hole injection is still necessary to ensure low noise in thin 4H-SiC APDs owing to large α_p/α_n ratios, even at very high fields.

IV. SINGLE PHOTON DETECTION

The 4H-SiC APDs may be biased for a short time above the breakdown to make them capable of detecting single incident photon [12-13]. This mode of operation of APDs are called Geiger mode. X. Bai *et al*. [4] characterized the single photon detection performance of the 4H-SiC APDs with a gated quenching circuit [13-15]. Significantly low dark count probability (8×10^{-4}) was achieved with 180 μm diameter 4H-SiC APDs. The defect densities of state of the art SiC dictate that larger photosensitive areas can only be achieved with arrays. They fabricated a 4×4 array with 75% yield for the experiment.

V. EFFECT OF ELECTRON VERSUS HOLE PHOTOCURRENT

The effect of electron versus hole photocurrent on the opto-electric properties such as responsivity, optical gain of 4H-SiC DDR, p^+-p-n-n^+ structured RAPDs are investigated by Acharyya *et al*. [3] in 2012. They have developed a double-iterative simulation technique to study the electric and opto-electric performance of the device under two different optical illumination configurations such as (a) Top Mounted (TM) and (b) Flip-Chip (FC). In case of TM structure UV light is assumed to incident on the p^+-layer and corresponding photocurrent becomes electron dominated; whereas in case of FC structure, UV light is assumed to shined on the n^+-layer of the device such that the photocurrent becomes hole dominated. The cross sectional views of the TM and FC structures are shown in Figure 1.

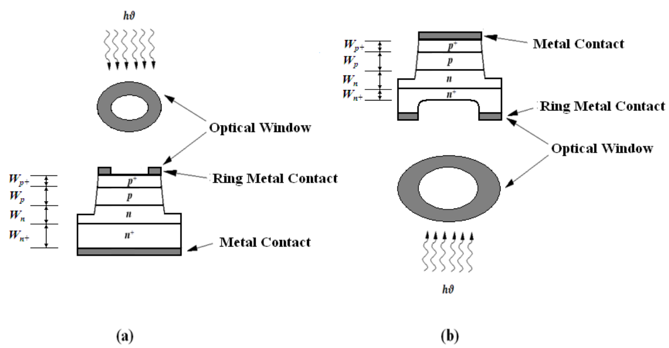

Figure 1: Cross-sectional view of the 4H-SiC reach-through DDR avalanche photodiodes for two optical illumination configurations (a) TM structure (top p^+-layer illuminated) and (b) FC structure (back n^+-layer illuminated).

One dimensional models of p^+-p-n-n^+ structured RAPDs in TM and FC configurations shown in Figure 2 are used for the simulation, since the physical phenomena takes place in the in the semiconductor bulk along the symmetry axis of the device. The static electric field profile and normalized current density ($P(x) = (J_n(x) - J_p(x)/J_T)$; where $J_T = J_p(x) + J_n(x)$) profiles of the device are obtained from the simultaneous numerical solution of the fundamental device equations such as Poisson's equation, combined carrier continuity equations in steady-state, current density equations and mobile space charge equation subject to appropriate boundary conditions [3]. The boundary conditions for the electric field at the depletion layer edges are given by:

$$\xi\left(x = W_{D_n}\right) = 0 \quad \text{and} \quad \xi\left(x = W_{D_p}\right) = 0$$

when light is illuminated on the n^+-layer (1 (a))

$$\xi\left(x = W_{D_p}{}'\right) = 0 \quad \text{and} \quad \xi\left(x = W_{D_n}{}'\right) = 0$$

when light is illuminated on the p^+-layer. (1 (b))

Similarly the boundary conditions (unilluminated device) for normalized current density at the depletion layer edges are given by:

$$P\left(x = W_{D_n}\right) = \left(\frac{2}{M_p\left(x = W_{D_n}\right)} - 1\right) \quad \text{and} \quad P\left(x = W_{D_p}\right) = \left(1 - \frac{2}{M_n\left(x = W_{D_p}\right)}\right)$$

when light is illuminated on the n^+-layer (2 (a))

$$P\left(x = W_{D_p}{}'\right) = \left(1 - \frac{2}{M_n\left(x = W_{D_p}{}'\right)}\right) \quad \text{and} \quad P\left(x = W_{D_n}{}'\right) = \left(\frac{2}{M_p\left(x = W_{D_n}{}'\right)} - 1\right)$$

when light is illuminated on the p^+-layer (2 (b))

where $M_n(x)$ and $M_p(x)$ are the position dependent electron and hole multiplication factors [3].

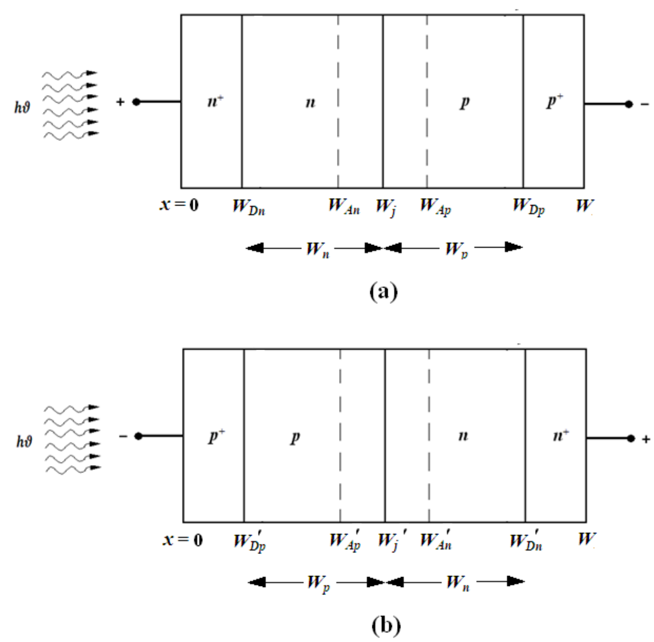

Figure 2: One-dimensional model of DDR APD under two optical illumination configurations i.e. (a) FC structure, (b) TM structure.

The drift components of the electron and hole photocurrent densities through the reverse biased DDR APDs due to incident optical power of P_{in} are given by:

$$J_{ps(Opt\ drift)} = -q \int_{W_{D_n}}^{W_{D_p}} G_L(x)\,dx$$

when light is illuminated on the n^+-layer (3)

$$J_{ns(Opt\ drift)} = -q \int_{W_{D_p}{}'}^{W_{D_n}{}'} G_L(x)\,dx$$

when light is illuminated on the p^+-layer (4)

where $G_L(x)$ is the electron-hole pair (EHP) generation rate. The electron and hole diffusion components of photo current density in both p^+- and n^+- layers are obtained by solving the one-dimensional diffusion equation with proper boundary conditions [16]. Those are given by:

$$J_{ns}(Opt\ \ diff) = qP_{in}\frac{(1-R(\lambda))\lambda}{Ahc}\left(\frac{\alpha(\lambda)L_n}{1+\alpha(\lambda)L_n}\right)exp\left(-\alpha(\lambda)W_{D_p}\right)$$

when light is illuminated on the n^+-layer (5)

$$J_{ps}(Opt\ \ diff) = qP_{in}\frac{(1-R(\lambda))\lambda}{Ahc}\left(\frac{\alpha(\lambda)L_p}{1+\alpha(\lambda)L_p}\right)exp\left(-\alpha(\lambda)W_{D_n}{}'\right)$$

when light is illuminated on the p^+-layer (6)

where $\alpha(\lambda)$ and $R(\lambda)$ are respectively the absorption coefficient and reflectance [$R = (n_2 - n_1)/(n_2 + n_1)$; n_2 = reflective index of the semiconductor, n_1 = refractive index of the air] of the semiconductor base material at a wavelength of λ , A is the illumination area of the device, h is the Planck's constant (h = 6.62×10^{-34} J s) , c is the velocity of the light in vacuum (c = 3.0×10^{8} m s^{-1}) and q is the unit electron charge ($q = 1.6\times10^{-19}$ C). For FC and TM structures, the electron and hole multiplication factors can be written as:

$$M_n\left(x=W_{D_p}\right)=\frac{J_T}{J_{ns(Th)}} \quad \text{and} \quad M_p{}'\left(x=W_{D_n}\right)=\frac{J_T}{J_{ps(Th)}+J_{ps(Opt)}}$$

in FC Structure (7)

$$M_n{}'\left(x=W_{D_p}{}'\right)=\frac{J_T}{J_{ns(Th)}+J_{ns(Opt)}} \quad \text{and} \quad M_p\left(x=W_{D_n}{}'\right)=\frac{J_T}{J_{ps(Th)}}$$

in TM Structure . (8)

Since in FC structure, UV light is shined on the n^+-side of the device and consequently the photocurrent density becomes hole dominated. On the other hand in TM structure, UV light is shined on the p^+-side of the device; as a result the photocurrent density becomes electron dominated. The normalized current density boundary conditions at the depletion layer edges (equations 2 (a) and 2 (b)) are modified to:

$$P\left(x=W_{D_n}\right)=\left(\frac{2}{M_p{}'\left(x=W_{D_n}\right)}-1\right) \text{ and } P\left(x=W_{D_p}\right)=1$$

in FC Structure (9)

$$P\left(x=W_{D_p}{}'\right)=\left(1-\frac{2}{M_n{}'\left(x=W_{D_p}{}'\right)}\right) \text{ and } P\left(x=W_{D_n}{}'\right)=-1$$

in TM Structure. (10)

In FC structure M_n is very large (~10^6) near the breakdown of the device and M_p is much smaller as compared to M_n under similar condition due to hole dominated photocurrent; whereas in TM structure M_n is considerably reduced due to electron dominated photocurrent while M_p remained unchanged (~10^6). Both the electrons and holes participate in the avalanche multiplication process in reverse biased DDR APDs near breakdown. Thus the mean value of avalanche multiplication factor can be expressed as:

$$M=\frac{I_M}{I_{ph}}=\frac{\left(M_pJ_{ps\_opt}+M_nJ_{ns\_opt}\right)}{\left(J_{ps\_opt}+J_{ns\_opt}\right)} \quad (11)$$

where I_M is the total multiplied photocurrent and I_{ph} is the total primary unmultiplied photocurrent. The responsivity $\Re$ (AW^{-1}) of a APD is defined as the output photocurrent per unit incident optical power [17-18]:

$$\Re=\frac{I_M}{P_{in}}=M\frac{I_{ph}}{P_{in}}=M.\Re_{unity\_gain} \quad (12)$$

where $\Re_{unity\_gain}$ is the unity gain responsivity of the device. Simulation is carried out to study the opto-electric performance of four DDR reach-through avalanche photo diodes based on 4H-SiC having different donor and acceptor doping levels in n-and p-layers respectively [3]. Multiplication factors are plotted against reverse bias voltage for FC and TM configurations at 260 nm wavelength in Figures 3 and 4 respectively.

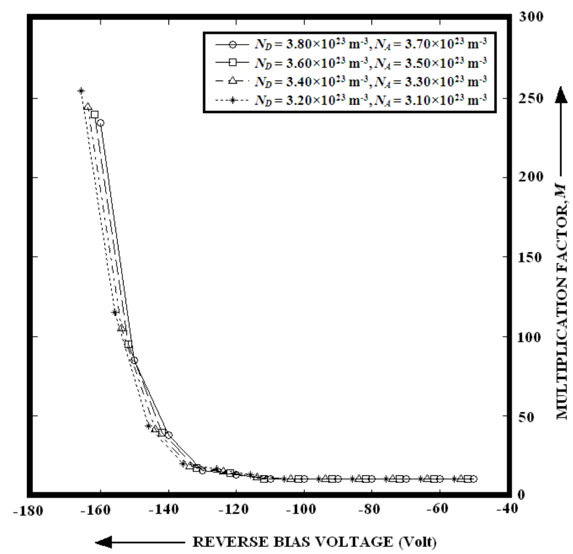

Figure 3: Variation of Multiplication Factor with Reverse Bias Voltage in DDR 4H-SiC RAPDs due to optical illuminated on the n^+-layer (FC structure).

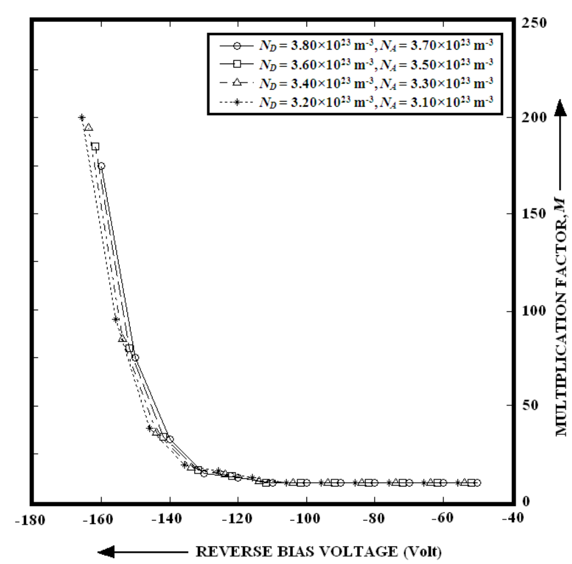

Figure 4: Variation of Multiplication Factor with Reverse Bias Voltage in DDR 4H-SiC RAPDs due to optical illuminated on the p^+-layer (TM structure).

It can be observed from Figures 3 and 4 that the peak multiplication factor near the breakdown is higher in FC structure (i.e. due to hole dominated photocurrent) as compared to that of TM structure (i.e. electron dominated photocurrent) [3]. It is also noteworthy that the multiplication factors i.e. the optical gain of the device increases as the doping levels of the *n*- and *p*-epitaxial layers are decreased, i.e. when the punch through factor of the device is higher. Lower doping level causes wider avalanche zone, which results higher avalanche multiplication.

Unity gain responsivity curves of DDR 4H-SiC APDs are shown in Figures 5 and 6 for FC and TM structures respectively [3]. Unity gain responsivity are calculated for the wavelength ranging from 210 to 350 nm and it is observed that peak unity gain responsivity is obtained at 260 nm for both optical illumination configurations (FC and TM). Again the peak unity gain responsivity is higher in FC structure (i.e. due to hole dominated photocurrent) as compared to TM structure (i.e. due to electron dominated photocurrent). Thus the above investigation shows that the photo sensitivity of 4H-SiC based DDR RAPDs is higher when the UV light is shined on the n^+-layer of the device (i.e. in FC structure) as compared to when the UV light is shined on the p^+-layer of the device (i.e. TM structure). Higher photo sensitivity of DDR 4H-SiC RADPs in hole dominated photocurrent is due to higher ionization rate of holes (α_p) as compared to that of electrons (α_n).

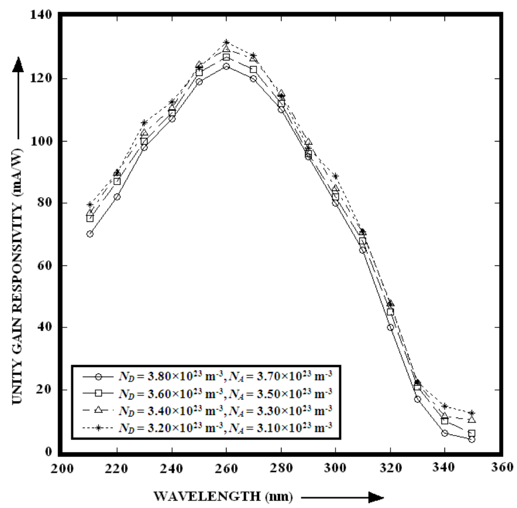

Figure 5: Variation of Unity Gain Spectral Responsivity with Wavelength in DDR 4H-SiC RAPDs due to optical illuminated on the n^+-layer (FC structure).

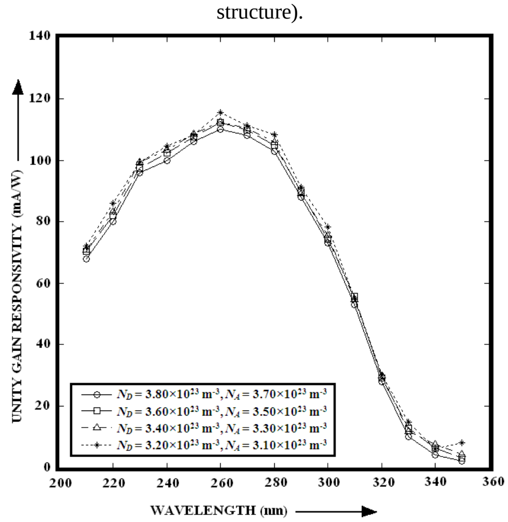

Figure 6: Variation of Unity Gain Spectral Responsivity with Wavelength in DDR 4H-SiC RAPDs due to optical illuminated on the p^+-layer (TM structure).

V. CONCLUSION

The prospects of 4H-SiC APDs as quality photodetectors which can be used in modern UV communication systems are briefly surveyed in this paper. The paper presents a concise review on several theoretical and experimental aspects of 4H-SiC APDs as visible-blind and near visible-blind UV sensors which can be an extremely fruitful guideline for the future researchers in this field for further advancements.

Acknowledgement

The authors would like to thank Supreme Knowledge Foundation Group of Institutions, Sir J. C. Bose School of Engineering, Mankundu, Hooghly, W. B., India for providing a healthy research environment and excellent learning facilities. Aritra Acharyya would like to thank Professor (Dr.) J. P. Banerjee, Radio Physics and Electronics Department, University of Calcutta, Kolkata, India for sharing his insight into the field of solid-state semiconductor materials and devices.

References

[1] F. Yan, J. H. Zhao and G. H. Olsen, "Demonstration of the 4H-SiC avalanche photodiodes", Solid-State Electronics, **44**, 341 (2000).

[2] B. K. Ng, J. P. R. David, R. C. Tozer and G. J. Rees, F. Yan, J. H. Zhao and M. Weiner, "Nonlocal Effectsin Thin 4H-SiC UV Avalanche Photodiodes", IEEE Transactions on Electron Devices, **50**, 1724 (2003).

[3] A. Acharyya and J. P. Banerjee, "Design and simulation of silicon carbide poly-type double-drift region avalanche photodiodes for UV sensing", Journal of Optoelectronics and Advanced Materials, **14**, XXX (2012).

[4] X. Bai, D. McIntosh, H. D. Liu and J. C. Cambell, "High Single Photon Detection Efficiency 4H-SiC Avalanche Photodiodes", Proc. of SPIE: Advanced Photon Counting Techniques III, Orlando, FL, USA, April 13, (2009), 7320, pp 732001-1.

[5] M. P. Ulmer, R. M. McClintock, J. L. Pau and M. Razeghi, "Advances in APDs for UV astronomy", Proc. of SPIE: UV, X-Ray, and Gamma-Ray Space Instrumentation for Astronomy XV, San Diego, CA, USA, August 26, (2007), 6686, pp 668605-1.

[6] M. Dehghan, V. Ahmadi and E. Darabi, "Investigation and analysis of time response in Geiger mode avalanche photodiode", Optica Applicata, **XL(2)**, 471 (2010).

[7] H. Mokari and M. H. Seyedi, "Numerical Analysis of Honojunction Avalanche Photodiodes (APDs)", Progress in Electromagnetics Research C, **3**, 45 (2008).

[8] W. Wu, A. R. Howkins and J. E. Bowers, "Frequency response of avalanche photodetectors with separate absorption and multiplication layers", Journal of Lighwave Technology, **14**, 2778 (1996).

[9] H. Mokari and P. D. Barjoei, "Numerical Analysis Homojunction Gallium Arsenide Avalanche Photodiodes (GaAs-APDs)", Progress in Electromagnetics Research B, **7**, 159 (2008).

[10] I. Wegrzecka, M. Wegrzecki, M. Grynglas, J. Bar, A. Uszynski, R. Grodecki, P. Grabiec, S. Krzeminski and T. Budzynski, "Design and properties of silicon avalanche photodiodes", Opto-Electronics Review, **12**, 95 (2004).
[11] D. M. Brown, E. T. Downey, M. Ghezzo, J. W. Kretchmer, R. J. Saia, Y. S. Liu *et al*., "Silicon carbide UV photodiodes", IEEE Transactions on Electron Devices, **40**, 325 (1993).
[12] X. Bai, D. McIntosh, H. D. Liu and J. C. Cambell, "Ultraviolet Single Photon Detection with Geiger-mode 4H-SiC Avalanche Photodiodes", IEEE Photonics Technol. Lett., **19**, 1822 (2007).
[13] A.L. Beck, X. Guo, H. Liu, A. Ghatakroy and J. C. Cambell, "Low dark count rate 4H-SiC Geiger mode avalanche photodiodes operated under gated quenching at 325 nm", Proc. of SPIE: Advanced Photon Counting Techniques, Boston, MA, USA, October 1, 2006, 6372, 63720O.
[14] S. Cova, M. Ghioni, A. Lacaita, C. Samori, F. Zappa, "Avalanche photodiodes and quenching circuits for single-photon detection", Applied Optics, **35**, 1956 (1996).
[15] M. Liu, X. Bai, C. Hu, X. Guo, J. C. Campbell, "Low dark count rate and high single-photon detection efficiency avalanche photodiode in Geiger-mode operation", IEEE Photonics Technol. Lett., **19**, 378 (2007).
[16] S. M. Sze, Kwok K. Ng, Physics of Semiconductor Devices, Willy-India: 3rd Edition, India (2010).
[17] R. P. Khare, Fiber Optics and Optoelectronics, Oxford University Press, New York, USA (2006).
[18] J. M. Senior, Optical Fiber Communications, Pearson Education: 2nd Edition, India (2007).